

Vanilla Inflation Predicts Negative Running

Jérôme Martin,^{1,*} Christophe Ringeval,^{2,1,†} and Vincent Vennin^{3,1,‡}

¹*Institut d'Astrophysique de Paris, 98bis boulevard Arago, 75014 Paris, France*

²*Cosmology, Universe and Relativity at Louvain (CURL),*

Institute of Mathematics and Physics, University of Louvain,

2 Chemin du Cyclotron, 1348 Louvain-la-Neuve, Belgium

³*Laboratoire de Physique de l'École Normale Supérieure, ENS, CNRS, Université PSL, Sorbonne Université, Université Paris Cité, 75005 Paris, France*

(Dated: August 30, 2024)

We show that the simplest, and currently favoured, theoretical realizations of cosmic inflation yield a sharp prediction for the running of the spectral index α_s . Using latest cosmological data, we compute its marginalized posterior probability distribution over the space of nearly 300 models of single-field slow-roll inflation. The most probable value is $\alpha_s = -6.3 \times 10^{-4}$, lying within the 98% credible interval $-1.8 \times 10^{-3} < \alpha_s < -9.1 \times 10^{-5}$. Within the landscape of all the proposed slow-roll inflationary models, positive values for the running are therefore disfavoured at more than three-sigma.

INTRODUCTION

Cosmic inflation is an epoch of accelerated expansion that took place in the very early Universe, prior to the eras described by the hot Big-Bang model. The main motivation for introducing this new phase of evolution is that the resulting framework becomes free of the various puzzles that plague the standard cosmological model. Inflation comes in different incarnations but, at least for the moment, the simplest realization, where inflation is driven by a single scalar field with a minimal kinetic term (the so-called inflaton field ϕ), is sufficient to explain the cosmological data. The mere existence of inflation addresses the smallness of the spatial curvature today, the Gaussian statistics of the Cosmic Microwave Background (CMB) anisotropies, the adiabaticity of the initial conditions, and the presence of a nearly scale-invariant primordial power spectrum \mathcal{P}_ζ for curvature perturbations. This last property has a special status as it was a prediction of inflation (in contrast to a postdiction), which was recently verified at a significant statistical level. Deviations from scale-invariance are encoded in the value of the so-called spectral index, n_s , evaluated at a pivot wavenumber k_*

$$n_s - 1 \equiv \left. \frac{d \ln [\mathcal{P}_\zeta(k)]}{d \ln k} \right|_{k=k_*}. \quad (1)$$

The latest cosmological data give, at $k_* = 0.05 \text{ Mpc}^{-1}$, $n_s = 0.9649 \pm 0.004$ at 68% confidence limit [1]. Because $n_s < 1$, the primordial power spectrum $\mathcal{P}_\zeta(k)$ is slightly red, i.e., there is slightly more power at low wavenumbers k than at high wavenumbers.

There are different ways of understanding why the simplest single-field slow-roll scenarios mentioned above are associated with $n_s \lesssim 1$. Indeed, typically for this class of models, the potential $V(\phi)$ of the inflaton field is monotonous and, as inflation proceeds, it becomes increasingly steep. As a consequence, the inflaton accelerates

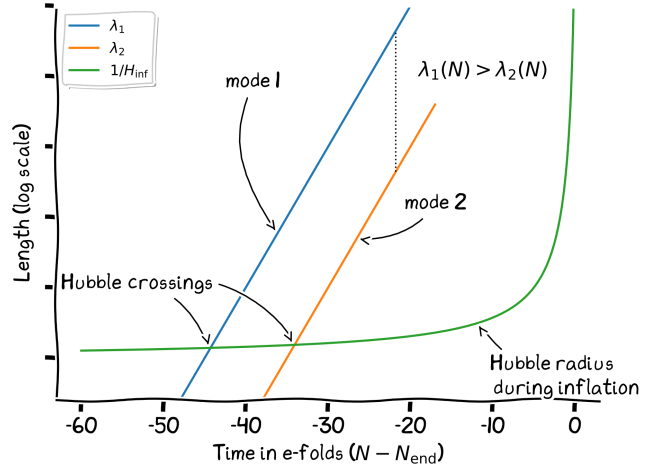


FIG. 1: Evolution of two cosmological perturbations, of wavelengths λ_1 and λ_2 , during cosmic inflation. Their amplitude is proportional to $H/\sqrt{\epsilon_1}$, evaluated at Hubble crossing, i.e., when the wavelength equals the distance to the event horizon. In such a simple scenario, one has $n_s \lesssim 1$ together with $\alpha_s \lesssim 0$.

ates and the kinetic energy grows compared to the total energy so that, after a sufficient number of e -folds, denoted $N = \ln a$, inflation comes to an end. This means that the Hubble-flow functions, defined by [2, 3]

$$\epsilon_{i+1}(N) \equiv \frac{d \ln |\epsilon_i|}{dN}, \quad \epsilon_0(N) = \frac{M_{\text{P}}}{H}, \quad (2)$$

are typically increasing functions of time as inflation proceeds. For instance, the physical process described above implies that

$$\epsilon_1 = \frac{1}{2M_{\text{P}}^2} \left(\frac{d\phi}{dN} \right)^2, \quad (3)$$

grows, which means that $\epsilon_2 > 0$ thanks to Eq. (2). At leading order in the Hubble-flow functions, one can show [4–9] that the tensor-to-scalar ratio r is given by $r = 16\epsilon_1$ and $n_s - 1 \simeq -r/8 - \epsilon_2$. Given that primordial gravitational waves have not been detected, current cosmological data only set the upper bound $\log(\epsilon_1) < -2.6$ (95%) [10], which immediately implies that $n_s - 1 \simeq -\epsilon_2$, that is to say a red spectrum. From the value of $n_s \simeq 0.9649$ reported earlier, one has $\epsilon_2 \simeq 0.035$.

Another way to describe the same mechanism in simple terms is to remark that the amplitude of the power spectrum is given by $\mathcal{P}_\zeta(k) \propto H^2/(M_p^2\epsilon_1)$, evaluated when the mode k crosses out the Hubble radius. When inflation proceeds, H slightly decreases (since $H^2 \propto \rho$ can only decrease in an expanding universe) while ϵ_1 increases (if inflation, corresponding to $\epsilon_1 < 1$, ends by slow-roll violation when ϵ_1 reaches unity). As a result, at late times, the amplitude of the mode $\lambda_2 < \lambda_1$ is slightly lower than the one of λ_1 , see Fig. 1. This implies that $\mathcal{P}_\zeta(k_2) < \mathcal{P}_\zeta(k_1)$ with $k_2 > k_1$: this is a red tilt.

A red tilt is thus typically expected if inflation is described by vanilla models. In fact, the previous reasoning can be pushed one step further. Indeed, in the same context, the running of the spectral index is given by

$$\alpha_s \equiv \left. \frac{d^2 \ln [\mathcal{P}_\zeta(k)]}{d(\ln k)^2} \right|_{k=k_*} \simeq -\epsilon_2 (2\epsilon_1 + \epsilon_3), \quad (4)$$

and, therefore, a positive third Hubble-flow function $\epsilon_3 > 0$ implies a negative running. As such, one should expect the simplest single-field scenarios to exhibit both $n_s \lesssim 1$ and $\alpha_s \lesssim 0$. It is important to notice that inflationary models having $\alpha_s > 0$ do exist, in the same manner than there are models with $n_s \geq 1$. The main point here is that, within the aforementioned simplest picture, there must be a strong correlation between the value of n_s and α_s . Because the current data strongly constrain $n_s < 1$, one should be able to have a definite prediction for $\alpha_s < 0$, would the simplest scenarios be correct.

In the following, we quantitatively implement this idea and derive the posterior probability distribution for α_s given all the explicit theoretical realizations of slow-roll single-field inflation and using current cosmological data from both CMB and Baryonic Acoustic Oscillations (BAO).

METHOD

We consider the space \mathcal{I}_{mod} of the single-field slow-roll inflationary models studied in Ref. [11], which amounts to 286 different scenarios. Each scenario, say \mathcal{M}_i , comes with some primordial model parameters θ_p and their associated prior $\pi_i(\theta_p) = P(\theta_p|\mathcal{M}_i)$. The set $\{\theta_p\}$ is made of the parameters entering the shape of the potential $V(\phi)$, the parameters describing the reheating era after

inflation, and any other parameters specific to the scenario \mathcal{M}_i under scrutiny. A detailed description of each of these models, parameters, and priors, can be found in Refs. [10–12]. Moreover, we assume that, after the reheating, the universe evolves according to the Λ CDM model, which is described by the standard cosmological parameters, say θ_s . Given some cosmological data sets \mathcal{D} , and a likelihood functional $\mathcal{L}(\mathcal{D}|\theta_p, \theta_s, \mathcal{M}_i)$, one can determine the posterior probability distribution of all parameters

$$P(\theta_p, \theta_s|\mathcal{D}, \mathcal{M}_i) = \frac{\mathcal{L}(\mathcal{D}|\theta_p, \theta_s, \mathcal{M}_i) \pi_i(\theta_p) \pi(\theta_s)}{\mathcal{E}(\mathcal{D}|\mathcal{M}_i)}, \quad (5)$$

where the normalization constant is the Bayesian evidence

$$\mathcal{E}(\mathcal{D}|\mathcal{M}_i) = \int \mathcal{L}(\mathcal{D}|\theta_p, \theta_s, \mathcal{M}_i) \pi_i(\theta_p) \pi(\theta_s) d\theta_p d\theta_s. \quad (6)$$

The probability of model \mathcal{M}_i to explain the data is then given by

$$P(\mathcal{M}_i|\mathcal{D}, \mathcal{I}_{\text{mod}}) = \frac{\mathcal{E}(\mathcal{D}|\mathcal{M}_i) \pi(\mathcal{M}_i)}{P(\mathcal{D})}, \quad (7)$$

where $P(\mathcal{D})$ is a model-independent normalization factor and $\pi(\mathcal{M}_i) = P(\mathcal{M}_i|\mathcal{I}_{\text{mod}})$ is the prior probability of model \mathcal{M}_i within the space \mathcal{I}_{mod} . In the following, we consider non-committal priors, i.e., $\pi(\mathcal{M}_i) = 1/286$ for all models.

For all \mathcal{M}_i , the Hubble-flow functions $\epsilon_i(\theta_p)$ are known, and, from Eq. (4), one can derive the running of the spectral index $\alpha_s(\theta_p)$ ¹. All the posteriors $P(\theta_p|\mathcal{D}, \mathcal{M}_i)$ can be obtained by performing separated data analysis of \mathcal{D} given \mathcal{M}_i , and, from these, it is straightforward to derive the posteriors of α_s given \mathcal{M}_i ,

$$P(\alpha_s|\mathcal{D}, \mathcal{M}_i) = \int P(\theta_p|\mathcal{D}, \mathcal{M}_i) \delta[\alpha_s - \alpha_s(\theta_p)] d\theta_p. \quad (8)$$

We can then marginalize over all models \mathcal{M}_i filling the space \mathcal{I}_{mod} to obtain

$$P(\alpha_s|\mathcal{D}, \mathcal{I}_{\text{mod}}) = \sum_i P(\alpha_s|\mathcal{D}, \mathcal{M}_i) P(\mathcal{M}_i|\mathcal{D}), \quad (9)$$

where $P(\mathcal{M}_i|\mathcal{D})$ is given by Eq. (7). Let us notice that each posterior appears weighted by the probability of the associated model, ensuring that the most disfavoured scenarios have almost no effect on the final result. The posterior probability distribution $P(\alpha_s|\mathcal{D}, \mathcal{I}_{\text{mod}})$ is the quantity of interest: it is quantifying how probable a given value of the running is given both the data sets \mathcal{D} and the space of all models \mathcal{I}_{mod} .

¹ In practice, we have used the public library `ASPIC` to compute the Hubble-flow functions and the running [13].

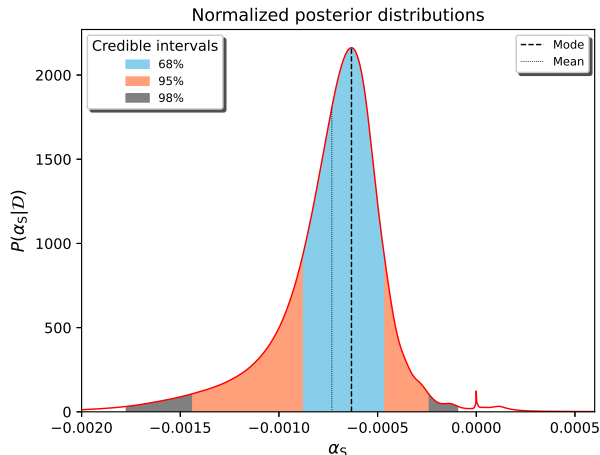


FIG. 2: Posterior probability distribution for the running of the spectral index α_s marginalized over 286 slow-roll inflationary models. Shaded regions show various annotated credible intervals comprising the mode and the mean value. Positive values of the running are disfavoured at more than three-sigma.

RESULTS

The data sets \mathbf{D} used are the 2020 post-legacy release of the Planck satellite CMB data [14–18], complemented with the BICEP/Keck array 2021 data [19], the South Pole Telescope third generation measurements [20] and a compilation of BAO data from the Sloan Digital Sky Survey IV [21, 22]. Data analysis has been done using modified versions of the CAMB and COSMOMC codes [23, 24] to machine-learn an effective likelihood [25] which is fed to the PolyChord code [26, 27]. The latter code is used to perform fast nested sampling and evidence computation for the 286 models. The details of this analysis can be found in Ref. [10].

Our main result is $P(\alpha_s|\mathbf{D}, \mathcal{I}_{\text{mod}})$, which is represented in Fig. 2. The maximum and the mean value of the running, a posteriori, are given by

$$\alpha_s|_{\text{max}} = -6.3 \times 10^{-4}, \quad \langle \alpha_s \rangle = -7.3 \times 10^{-4}, \quad (10)$$

respectively. They are both located within the following credible intervals

$$\begin{aligned} -8.8 \times 10^{-4} < \alpha_s < -4.7 \times 10^{-4} & \quad (68\%), \\ -1.4 \times 10^{-3} < \alpha_s < -2.4 \times 10^{-4} & \quad (95\%), \\ -1.8 \times 10^{-3} < \alpha_s < -9.1 \times 10^{-5} & \quad (98\%), \end{aligned} \quad (11)$$

which are represented as shaded regions in Fig. 2. The posterior $P(\alpha_s|\mathbf{D}, \mathcal{I}_{\text{mod}})$ is almost vanishing in the positive domain $\alpha_s > 0$ and this implies that, indeed, all single-field slow-roll models fitting well the current cosmological data are associated with negative running.

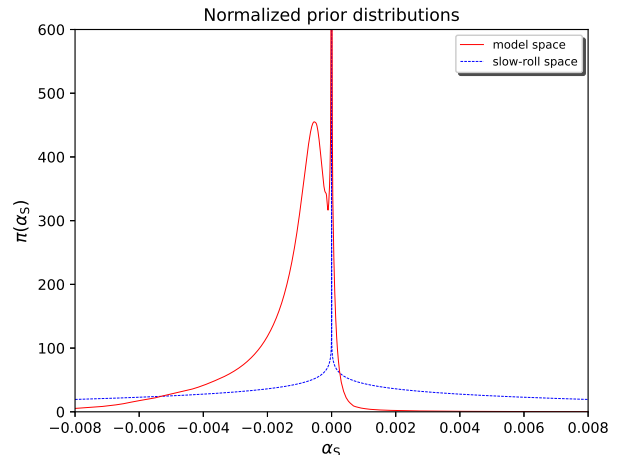


FIG. 3: Prior probability distributions for the running of the spectral index α_s . The solid red curve is within \mathcal{I}_{mod} , marginalized over 286 slow-roll inflationary models \mathcal{M}_i and assuming non-committal priors $\pi(\mathcal{M}_i) = 1/286$. The blue dashed curve is the prior distribution assuming only slow-roll power spectra and standard priors on the Hubble-flow functions (see text).

Let us insist that Eq. (10) and Eqs. (11) can be interpreted as predictions for α_s within the space \mathcal{I}_{mod} , i.e., the space filled with all the simplest theoretical implementations of single-field slow-roll inflation. If \mathcal{I}_{mod} is truly representative of the actual way inflation occurred, future data are going to match the figures quoted in Eq. (10) and Eqs. (11). On the contrary, measuring positive values of the running would imply that the simplest picture sketched in Fig. 1 is incorrect and the evolution of the Hubble radius has to be more complex than the one featured by vanilla models.

The data analysis we have presented is fully Bayesian, and, in order to emphasize the importance of Fig. 2, one also needs to discuss its dependence with respect to the priors.

DISCUSSION

The prior probability distribution of the running is $\pi_{\text{mod}}(\alpha_s) = P(\alpha_s|\mathcal{I}_{\text{mod}})$. From the previous discussion, it is given by the weighted sum of all prior distributions associated with the primordial parameters θ_p of each models \mathcal{M}_i . One has

$$\pi_{\text{mod}}(\alpha_s) = \sum_i \int \delta[\alpha_s - \alpha_s(\theta_p)] \pi_i(\theta_p) d\theta_p \pi(\mathcal{M}_i). \quad (12)$$

This distribution has been plotted in Fig. 3 as a red solid curve. It is not symmetric and negative values are clearly preferred. Again, this is because the single-field slow-roll

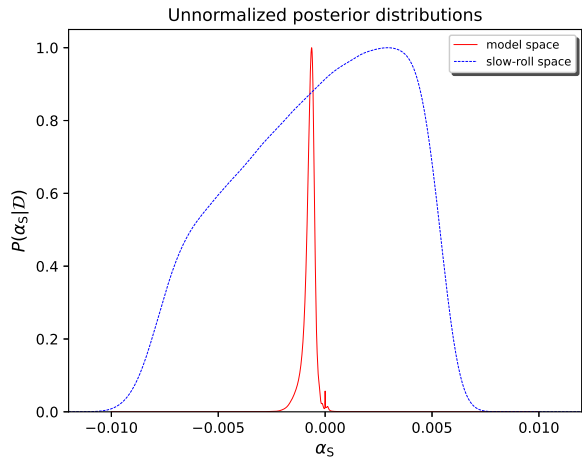


FIG. 4: Comparison between the posteriors $P(\alpha_s|\mathbf{D}, \mathcal{I}_{\text{mod}})$ (red solid) and $P(\alpha_s|\mathbf{D}, \mathcal{I}_{\text{sr}})$ (blue dashed). The former is associated with the space \mathcal{I}_{mod} of explicit theoretical realization of single-field slow-roll inflation whereas the latter, \mathcal{I}_{sr} , assumes only a Hubble-flow functional shape for the primordial power spectra. Explicit models, given the current data, are much more predictive.

models within \mathcal{I}_{mod} are mostly associated with smooth potentials and behave as sketched in Fig. 1. However, we should notice that there is a tail in the positive region, signalling that some models predict a positive running, and a sharp peak at vanishing α_s . This peak comes from a subclass of inflationary models having, for instance, a hilltop, or an inflection point, or very flat regions in which the field gets trapped and inflation may end by another mechanism than slow-roll violation. In this situation, inflation is very close to pure de Sitter, the Hubble radius is very close to constant and all Hubble-flow functions are very small. As a consequence, these models are making definite predictions: $n_s \simeq 1$ and $\alpha_s \simeq 0$, hence the peak. However, these de-Sitter like scenarios have been disfavoured since the first measurements of a red-tilted spectral index [28], and, as evident from Fig. 2, only a small peak at $\alpha_s = 0$ remains in the posterior $P(\alpha_s|\mathbf{D}, \mathcal{I}_{\text{mod}})$. Comparing the width of the prior in Fig. 3 to the posterior in Fig. 2, as well as the confidence intervals quoted in Eq. (11), it is clear that our constraints, within \mathcal{I}_{mod} , are significantly driven by the data and are non-trivial.

It is also informative to compare our results, applicable to \mathcal{I}_{mod} , to the ones that could be obtained starting from a much wider space in the realm of slow-roll inflation. Let us define \mathcal{I}_{sr} , the space of “just slow-roll” in which no explicit field theoretical realization is assumed. The hypothesis space \mathcal{I}_{sr} only assumes a slow-roll shape for the primordial power spectra, where $\mathcal{P}_\zeta(k)$ [and $\mathcal{P}_h(k)$ for tensors] are known functional of the Hubble-flow func-

tions ϵ_i (see, for instance, Refs. [29–31] for their explicit expression and derivation). From the motivated priors² $\log(\epsilon_1) \in [-5, -0.7]$, $\epsilon_2 \in [-0.2, 0.2]$ and $\epsilon_3 \in [-0.2, 0.2]$, Eq. (4) allows us to compute $\pi_{\text{sr}}(\alpha_s) \equiv P(\alpha_s|\mathcal{I}_{\text{sr}})$, which is plotted as a blue dashed curve in Fig. 3. It is a normalizable distribution sharply peaked at $\alpha_s = 0$, having very long tails. It is symmetric and does not favour positive nor negative values of α_s . Using the data sets \mathbf{D} described earlier, we have derived the posterior distribution $P(\alpha_s|\mathbf{D}, \mathcal{I}_{\text{sr}})$. It is represented in Fig. 4 as a blue dashed curve. For convenience, we have also reported the posterior $P(\alpha_s|\mathbf{D}, \mathcal{I}_{\text{mod}})$ as a solid red curve (same curve as in Fig. 2). This figure confirms that narrowing down the hypothesis space to \mathcal{I}_{mod} , i.e., performing data analysis within explicit theoretical realizations of single-field slow-roll inflation, significantly boosts the predictive power of the cosmological data.

What would it take to change our conclusion? First, inflation could have been realised by a *vanilla model* not pertaining to \mathcal{I}_{mod} . If a large number of new models having totally different runnings, fitting well the data³, were to be discovered, then our posterior distribution on the scalar running would be substantially revised. Although this seems unlikely, let us contemplate this possibility. The analysis of Ref. [10] reveals that many of the single-field models proposed after the release of the Planck 2013 data turn out to be disfavoured (between 2013 and today, the fraction of rejected models increased from 29 % to 41 %, although 112 additional models were included in the recent analysis). This goes against the common lore that theorists only propose models that are compatible with the data available to them, and that the predictions of these models reflect changes in the data rather than phenomenological typicality of a class of theories. Instead, we argue that the models that have already been proposed are representative of single-field constructions in general, and that negative running does constitute a typical prediction of vanilla inflation.

Second, one may want to work with *model priors* differing from the non-committal ones but, without a well-justified physical reason, this would certainly be viewed as an awkward approach. In fact, if one were to give more prior weight to models grounded in deeper theoretical motivations than to potential functions proceeding from more phenomenological parametrisations, one would exclude positive running with even higher statistical confidence.

Third, inflation could have occurred in a *non-vanilla model*. This would come with additional signatures (en-

² The first Hubble-flow function ϵ_1 is of unknown order of magnitude whereas all $|\epsilon_i|$ should be smaller than unity.

³ Otherwise their contribution to the running posterior will be suppressed by their Bayesian evidence.

tropic perturbations, non-Gaussianities, ...) that would significantly modify Bayesian model comparison. At this stage however, these signatures are constrained to be small by the data, hence the most conservative and minimal assumption is that single-field slow-roll inflation took place in the early universe. And this predicts negative running. We conclude that it would be worth targeting future observations [32, 33] to reach the figures quoted in Eq. (10) and Eqs. (11) to either confirm it, or, ruling it out.

We are indebted to Steven Gratton and Erik Rosenberg for having provided us with their latest `CamSpec` likelihood module for `COSMOMC`. This work is supported by the ESA Belgian Federal PRODEX Grant N°4000143201.

* Electronic address: jmartin@iap.fr

† Electronic address: christophe.ringeval@uclouvain.be

‡ Electronic address: vincent.vennin@ens.fr

- [1] Y. Akrami et al. (Planck), *Astron. Astrophys.* **641**, A10 (2020), 1807.06211.
- [2] D. J. Schwarz, C. A. Terrero-Escalante, and A. A. Garcia, *Phys. Lett.* **B517**, 243 (2001), astro-ph/0106020.
- [3] D. J. Schwarz and C. A. Terrero-Escalante, *JCAP* **0408**, 003 (2004), hep-ph/0403129.
- [4] E. D. Stewart and D. H. Lyth, *Phys. Lett.* **B302**, 171 (1993), gr-qc/9302019.
- [5] A. R. Liddle, P. Parsons, and J. D. Barrow, *Phys. Rev.* **D50**, 7222 (1994), astro-ph/9408015.
- [6] T. T. Nakamura and E. D. Stewart, *Phys. Lett.* **B381**, 413 (1996), astro-ph/9604103.
- [7] M. B. Hoffman and M. S. Turner, *Phys. Rev.* **D64**, 023506 (2001), astro-ph/0006321.
- [8] J.-O. Gong and E. D. Stewart, *Phys. Lett.* **B510**, 1 (2001), astro-ph/0101225.
- [9] S. M. Leach, A. R. Liddle, J. Martin, and D. J. Schwarz, *Phys. Rev.* **D66**, 023515 (2002), astro-ph/0202094.
- [10] J. Martin, C. Ringeval, and V. Vennin (2024), 2404.10647.
- [11] J. Martin, C. Ringeval, and V. Vennin, *Phys. Dark Univ.* **5-6**, 75 (2014), 1303.3787v3.
- [12] J. Martin, C. Ringeval, R. Trotta, and V. Vennin, *JCAP* **1403**, 039 (2014), 1312.3529.
- [13] J. Martin, C. Ringeval, and V. Vennin, *ASPIC: Accurate Slow-roll Predictions for Inflationary Cosmology*, Astrophysics Source Code Library, record ascl:1806.031 (2018), URL <https://github.com/cosmicinflation/aspic>.
- [14] N. Aghanim et al. (Planck), *Astron. Astrophys.* **641**, A5 (2020), 1907.12875.
- [15] G. Efstathiou and S. Gratton (2019), 1910.00483.
- [16] Y. Akrami et al. (Planck), *Astron. Astrophys.* **643**, A42 (2020), 2007.04997.
- [17] M. Tristram et al., *Astron. Astrophys.* **647**, A128 (2021), 2010.01139.
- [18] E. Rosenberg, S. Gratton, and G. Efstathiou, *Mon. Not. Roy. Astron. Soc.* **517**, 4620 (2022), 2205.10869.
- [19] P. A. R. Ade et al. (BICEP, Keck), *Phys. Rev. Lett.* **127**, 151301 (2021), 2110.00483.
- [20] D. Dutcher et al. (SPT-3G), *Phys. Rev. D* **104**, 022003 (2021), 2101.01684.
- [21] K. S. Dawson et al., *Astron. J.* **151**, 44 (2016), 1508.04473.
- [22] M. R. Blanton et al. (SDSS), *Astron. J.* **154**, 28 (2017), 1703.00052.
- [23] A. Lewis, A. Challinor, and A. Lasenby, *Astrophys. J.* **538**, 473 (2000), astro-ph/9911177.
- [24] A. Lewis and S. Bridle, *Phys. Rev.* **D66**, 103511 (2002), astro-ph/0205436.
- [25] C. Ringeval, *Mon. Not. Roy. Astron. Soc.* **439**, 3253 (2014), 1312.2347.
- [26] W. J. Handley, M. P. Hobson, and A. N. Lasenby, *MNRAS* **453**, 4384 (2015), 1506.00171.
- [27] W. J. Handley, M. P. Hobson, and A. N. Lasenby, *Mon. Not. Roy. Astron. Soc.* **450**, L61 (2015), 1502.01856.
- [28] C. L. Bennett, D. Larson, J. L. Weiland, N. Jarosik, G. Hinshaw, N. Odegard, K. M. Smith, R. S. Hill, B. Gold, M. Halpern, et al., *ApJS* **208**, 20 (2013), 1212.5225.
- [29] J. Martin, C. Ringeval, and V. Vennin, *JCAP* **1306**, 021 (2013), 1303.2120.
- [30] J. Beltran Jimenez, M. Musso, and C. Ringeval, *Phys. Rev.* **D88**, 043524 (2013), 1303.2788.
- [31] P. Auclair and C. Ringeval, *Phys. Rev. D* **106**, 063512 (2022), 2205.12608.
- [32] R. J. Hardwick, V. Vennin, and D. Wands, *JCAP* **05**, 070 (2018), 1803.09491.
- [33] R. Easter, B. Bahr-Kalus, and D. Parkinson (2021), 2112.10922.